Numerical Analysis of Cell Deformation of Two-phase Flow with Discontinuous Viscosity and Non-linear Surface Tension

Zhilin Li and Sharon Lubkin
Center For Research in Scientific Computation & Department of Mathematics
North Carolina State University, Raleigh, NC 27695-8205

September 10, 2000

keywords: Stokes equations, cell deformation, non-linear surface tension, jump conditions, interface, discontinuous and non-smooth solution, immersed interface method, cell cleavage

AMS Classification; 65M06, 65M12, 76T05

Abstract

In this paper, a fluid model of the incompressible Stokes equations is used to simulate the motion of a cell boundary separating two fluids that have equal or different viscosity and non-linear surface tension. Theoretically, our analysis lead to decoupled certain jump conditions that are used in constructing the numerical algorithm. Our numerical results agree with those in the literature and include some new results that may can be used to explain the cell cleavage process. The new method developed here preserves the area very well for our testing problems. Some interesting observations are obtained with different choices of the parameters.

1 Introduction

In the literature, the Stokes equations are widely used to simulate the deformation of cells, see [1, 2, 13] and many others.

In reality, cells live in mediums. Therefore quite often, a two phase model is reasonable. In this paper, we use the following Stokes equation with a periodic boundary condition to

study the motion of the fluids inside and outside of a cell.

$$\nabla p = \mu \Delta \mathbf{u}, \quad (x, y) \in \Omega - \Gamma, \tag{1.1}$$

$$\nabla \cdot \mathbf{u} = \mathbf{0}, \quad (x, y) \in \Omega, \tag{1.2}$$

$$\text{Periodic BC for } \mathbf{u} \text{ and } p, \tag{1.3}$$

where $\mathbf{u} = (u, v)$ is the velocity vector, p is the pressure, μ is the viscosity, which we assume to have constant value inside and outside of the cell, Ω is a bounded domain, Γ is the cell boundary which is closed and immersed in the domain, see Fig. 1 for an illustration. The periodic boundary condition is justified since the environment of cells does not vary very much and widely used for many biology problems, see [14, 15] and the references therein. Across the cell boundary, sometimes is called the interface, there are the following jump conditions

$$[p - 2\mu \left(\nabla u \cdot \mathbf{n}, \nabla v \cdot \mathbf{n}\right) \cdot \mathbf{n}] = \gamma(s)\kappa \tag{1.4}$$

$$[\mu \left(\nabla u \cdot \mathbf{n}, \nabla v \cdot \mathbf{n}\right) \cdot \tau] = -\frac{\partial \gamma(s)}{\partial \tau}, \tag{1.5}$$

where jump $[\cdot]$ is defined as the difference of the limiting value from outside of the cell boundary and that from the inside, $\mathbf{n}$ and τ are the unit normal pointing outwards, and tangential directions of the cell boundary respectively, $\gamma(s)$ is the surface tension which is the concentration of tension elements and is modeled as a separate equation in [1, 2]. In this paper, it does not have to be a constant but a function defined on the surface of the cell. The surface tension is the main driving force for the cell deformation. The boundary of the cell boundary has the same velocity as the fluids surrounding it:

$$\frac{\partial \Gamma}{\partial t} = \mathbf{u}. \tag{1.6}$$

Since the flow is viscous, the velocity is continuous across the cell boundary, see [4].

Almost all the numerical simulations for cell dynamics with a free boundary using the model of Stokes equations are based on a boundary integral method, see for example, [3, 16, 17] and some others. Little work can be found in the literature using the finite element method or the finite difference method to solve the problems because of the almost inhabited computational cost to solve the problem in the entire domain when the jump in the viscosity is large. However, when the viscosity is continuous, the problem can be solved easily with the finite difference method, see [8, 18] and others.

In this paper, we use a finite difference method based on a fast Poisson solver to solve the two-phase moving interface problem. One of advantages of this approach is that we able to obtain the velocity and pressure in the entire domain without sacrificing the speed of the simulation. The approach described here is not tied to a boundary integral equation which

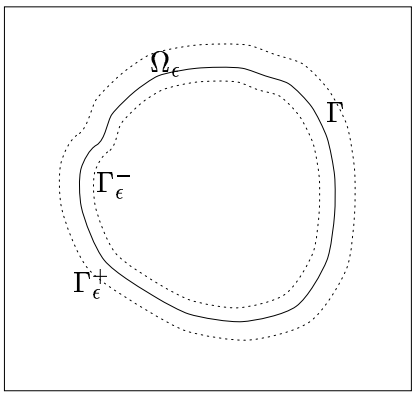

Figure 1: A diagram of the geometry discussed in this paper and it is used for the derivation of jump relations.

is useful to construct some desired force along the cell boundary to control the shape of the moving interface even if a boundary integral equation is not available or difficult to derive.

Outside and inside the domain excluding the boundary of the cell, the equations (1.1) can be reformulated as a sequence of three Poisson problems, one for each variable due to the incompressibility condition. For piecewise constant viscosity, applying the divergence operator to (1.1) and using the incompressibility condition, we get

$$\Delta p = 0, \quad (x, y) \in \Omega - \Gamma, \quad \text{periodic BC on } \partial\Omega \text{ for } p, \tag{1.7}$$

where Δ is the Laplacian operator. Since the right hand side is known, this is a Poisson problem for the pressure. Once p is known, the equations (1.1) represents two independent Poisson problems for u and v respectively. However the solutions outside and inside are not independent. A numerical algorithm that ignores the coupling relations usually lower the accuracy especially at or near the interface. In this paper, we derive the jump conditions of the solution across the cell boundary and use them to construct accurate solution method.

The rest of the paper is organized as follows. In Section 2, we derive the jump conditions for (1.1)-(1.3). In Section 3, we outline our numerical algorithm which is rather straightforward if we know the jump conditions. Numerical experiments are provided and analyzed in Section 4. Some conclusions will be given in Section 5.

2 Decoupling the jump conditions.

Using the immersed interface method (IIM), [7, 9, 10, 11, 12], we can solve the three Poisson equation efficiently if we know the jump conditions in the solution and in the flux. However, the jump conditions given in (1.4)-(1.5) are coupled and we can not use them directly. The approach used in [8] for Stokes equation can not be applied due to the discontinuity in the viscosity. Fortunately, the following theorem gives decoupled jump conditions.

Theorem 1 *Let p, u, and v be the solution of (1.1)-(1.3) with the jump conditions (1.4)-(1.5). Then the following equalities hold*

$$[\mu \mathbf{u_n}] = \frac{\partial \gamma(s)}{\partial \tau}\,\tau, \tag{2.8}$$

$$[p] = \gamma(s)\,\kappa, \tag{2.9}$$

$$[p_{\mathbf{n}}] = \frac{\partial^2 \gamma}{\partial \tau^2}. \tag{2.10}$$

It is more convenient to use the local coordinates to prove this theorem. Let (X, Y) be a point on the interface, and the unit normal and tangential directions are

$$\mathbf{n} = (\cos\theta, \sin\theta), \qquad \tau = (-\sin\theta, \cos\theta)$$

respectively, where θ is the angle between the outward normal direction and the x-axis, see Fig. 2 for an illustration. The local coordinates at (X, Y) then is

$$\begin{aligned} \xi &= (x - X)\cos\theta + (y - Y)\sin\theta, \\ \eta &= -(x - X)\sin\theta + (y - Y)\cos\theta. \end{aligned} \tag{2.11}$$

We first we prove the following lemma which is needed in the proof of Theorem 1.

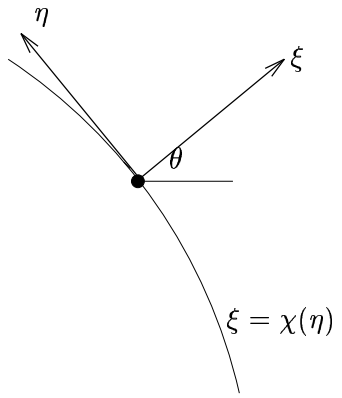

Figure 2: Local coordinates and geometry.

Lemma 1 *Let* $\mathbf{u}$ *be the solution to (1.1)-(1.3). Then the following equalities are true.*

$$[\,\mu\,(u_{xx} + v_{xy})\,] = 0, \qquad [\,\mu\,(u_{xy} + v_{yy})\,] = 0, \tag{2.12}$$

$$[\,\mu u_x \cos\theta + v_x \sin\theta\,] = 0, \qquad [\,\mu u_y \cos\theta + v_y \sin\theta\,] = 0. \tag{2.13}$$

Proof: In the inside and outside of the domain excluding the interface, we have

$$\begin{aligned} &u_x + v_y = 0, \quad \text{and} \quad \mu\,(u_x + v_y) = 0, \\ &\mu\,(u_{xx} + v_{xy}) = 0, \quad \text{and} \quad \mu\,(u_{xy} + v_{yy}) = 0. \end{aligned}$$

Therefore we can continuous extend the definitions above to everywhere inside the domain Ω and we have the equalities in (2.12) right way.

To prove the second part, we enclose the interface with a small domain $\Omega(\epsilon)$, see Fig. 1 for an illustration. Let $\phi(x,y) \in C^\infty$ be a two dimensional testing function. Since $\mu\,(u_{xx}+v_{xy})$ and $\mu\,(u_{xy}+v_{yy})$ are continuous inside $\Omega(\epsilon)$ after the extension, we have

$$\mu\,(u_{xx}+v_{xy}) = \nabla\cdot\mu\begin{bmatrix} u_x \\ \\ v_x \end{bmatrix} = 0, \tag{2.14}$$

$$\mu\,(u_{xy}+v_{yy}) = \nabla\cdot\mu\begin{bmatrix} u_y \\ \\ v_y \end{bmatrix} = 0. \tag{2.15}$$

Here we have used the fact the μ is piecewise constant and

$$\mu(u_{xx}+v_{xy}) = \frac{\partial}{\partial x}\left(\mu\frac{\partial u}{\partial x}\right) + \frac{\partial}{\partial x}\left(\mu\frac{\partial v}{\partial yx}\right) = 0$$

has continuous extension across the cell boundary. Multiply (2.14) by any testing function $\phi(x,y) \in C^\infty(\Omega)$ and integrate over Ω_ϵ, from Green's theorem, we have

$$\begin{aligned}\lim_{\epsilon\to 0}\iint_{\Omega_\epsilon}\phi\mu\nabla\cdot\begin{bmatrix} u_x \\ \\ v_x \end{bmatrix}dxdy &= \int_\Gamma \phi\left[\mu\left(u_x\cos\theta + v_x\sin\theta\right)\right]ds + \lim_{\epsilon\to 0}\iint_{\Omega_\epsilon}\mu\nabla\phi\cdot\begin{bmatrix} u_x \\ \\ v_x \end{bmatrix}dxdy \\ &= \int_\Gamma \phi\left[\mu\left(u_x\cos\theta + v_x\sin\theta\right)\right]ds, \\ &= 0\end{aligned}$$

where we have used the fact that u_x and v_x are bounded. Since ϕ is arbitrary, we conclude that

$$\left[\mu\left(u_x\cos\theta + v_x\sin\theta\right)\right] = 0. \tag{2.16}$$

Similarly, we can get

$$\left[\mu\left(u_y\cos\theta + v_y\sin\theta\right)\right] = 0. \tag{2.17}$$

That completes the proof of the lemma.

Proof of Theorem 1. Expressing the jump condition (1.5) in terms of the local coordinates, we get:

$$-\sin\theta[\mu u_\xi] + \cos\theta[\mu v_\xi] + \cos\theta[\mu u_\eta] + \sin\theta[\mu v_\eta] = -\frac{\partial\gamma(s)}{\partial\tau}. \tag{2.18}$$

Expressing the jump condition $[\mu(u_x+v_y)] = 0$ in terms of the local coordinates, we have:

$$\cos\theta[\mu u_\xi] + \sin\theta[\mu v_\xi] + -\sin\theta[\mu u_\eta] + \cos\theta[\mu v_\eta] = 0 \tag{2.19}$$

Under the local coordinates, the two equalities in (2.13) are:

$$\cos^2\theta[\mu u_\xi] + \sin\theta\cos\theta[\mu v_\xi] - \sin\theta\cos\theta[\mu u_\eta] - \sin^2\theta[\mu v_\eta] = 0, \tag{2.20}$$

$$\sin\theta\cos\theta[\mu u_\xi] + \sin^2\theta[\mu v_\xi] + \cos^2\theta[\mu u_\eta] + \sin\theta\cos\theta[\mu v_\eta] = 0. \tag{2.21}$$

The coefficient matrix of (2.18)-(2.21) is non-singular whose inverse evaluated using Maple is:

$$\begin{bmatrix} -\sin\theta & 0 & 2\cos^2\theta - 1 & 2\sin\theta\cos\theta \\ \cos\theta & 0 & 2\sin\theta\cos\theta & -2\cos^2\theta + 1 \\ 0 & -\sin\theta & 0 & 1 \\ 0 & \cos\theta & -1 & 0 \end{bmatrix}. \tag{2.22}$$

Therefore we have proved that

$$[\mu u_\xi] = -\frac{\partial\gamma}{\partial\tau}\sin\theta, \qquad [\mu v_\xi] = \frac{\partial\gamma}{\partial\tau}\cos\theta,$$

which is (2.8) in Theorem 1. The proof of (2.9) is straightforward if we substitute the equalities above into (1.4).

From the system of equations and the inverse of the coefficient matrix, we also conclude that

$$[\mu u_\eta] = 0, \qquad [\mu v_\eta] = 0.$$

Let the interface Γ be $\xi = \chi(\eta)$ in the neighborhood of $(\xi, \eta) = (0, 0)$, which satisfies $\chi(0) = 0$, $\chi'(0) = 0$. Then $\chi''(0) = \kappa$, the curvature of the interface at $(0, 0)$. Differentiating $[\mathbf{u}_\eta] = \mathbf{0}$ along the tangential direction, we get

$$[\mu u_{\eta\eta}] = 0, \qquad [\mu v_{\eta\eta}] = 0. \tag{2.23}$$

Differentiating $[\mu \mathbf{u}_\xi] = \frac{\partial\gamma}{\partial\tau}\tau$ along the tangential direction, we get

$$[\mu u_{\xi\eta}] = \frac{\partial^2\gamma}{\partial\tau^2}\tau + \kappa\frac{\partial\gamma}{\partial\tau}\mathbf{n}. \tag{2.24}$$

Expressing $[\mu(u_{xx} + v_{xy})] = 0$ and $[\mu(u_{xy} + v_{yy})] = 0$ in the local coordinates, we obtain

$$\begin{aligned} [\,\mu\,\big(&u_{\xi\xi}\cos^2\theta - 2u_{\xi\eta}\cos\theta\sin\theta + u_{\eta\eta}\sin^2\theta + v_{\xi\xi}\cos\theta\sin\theta \\ &+ v_{\xi\eta}(\cos^2\theta - \sin^2\theta) - v_{\eta\eta}\cos\theta\sin\theta\,\big)\,] = 0, \\ [\,\mu\,\big(&u_{\xi\xi}\cos\theta\sin\theta + u_{\xi\eta}(\cos^2\theta - \sin^2\theta) - u_{\eta\eta}\cos\theta\sin\theta \\ &+ v_{\xi\xi}\sin^2\theta + 2v_{\xi\eta}\cos\theta\sin\theta + v_{\eta\eta}\cos^2\theta\,\big)\,] = 0. \end{aligned}$$

Multiplying $\cos\theta$ to the first equation and $\sin\theta$ to the second equation above, after some algebra, we get

$$[\,\mu\,(u_{\xi\xi}\cos\theta + v_{\xi\xi}\sin\theta)\,] = [\,\mu\,(u_{\xi\eta}\sin\theta - v_{\xi\eta}\cos\theta)\,]. \tag{2.25}$$

Now we are ready to derive the jump condition for $\frac{\partial p}{\partial \mathbf{n}}$ from the momentum equation in the local coordinates:

$$\begin{aligned}
[\,\nabla p\cdot\mathbf{n}\,] &= [\,\mu\,(u_{\xi\xi}+u_{\eta\eta})\,]\cos\theta + [\,\mu\,(v_{\xi\xi}+v_{\eta\eta})\,]\sin\theta \\
&= [\,\mu\,(u_{\xi\eta}\sin\theta - v_{\xi\eta}\cos\theta)\,] \\
&= \frac{\partial^2\gamma}{\partial\tau^2}\sin^2\theta - \kappa\frac{\partial\gamma}{\partial\tau}\sin\theta\cos\theta + \frac{\partial^2\gamma}{\partial\tau^2}\cos^2\theta + \kappa\frac{\partial\gamma}{\partial\tau}\sin\theta\cos\theta \\
&= \frac{\partial^2\gamma}{\partial\tau^2}.
\end{aligned}$$

This completes the proof of Theorem 1.

Remark 1 *If we denote*

$$\hat{f}_1 = \gamma, \qquad \hat{f}_2 = \frac{\partial\gamma}{\partial\tau} \tag{2.26}$$

as the normal and tangential force strength, then the jump conditions proved in the theorem are the exact the same as those derived in [5, 8] for continuous viscosity.

3 Numerical method

For simplicity, we assume that the domain Ω is a rectangle $[a,\ b]\times[c,\ d]$, and the spatial spacing is $h = (b-a)/M = (d-c)/N$, where M and N are the number of grid points in the x and y directions, respectively. A standard uniform grid is used but the scheme discussed in this section can be generated to other grids as well without substantial difficulty.

We use a marked particle approach to express the moving interface since we are not particular interested in topological changes at this stage. The advantages using the particle approach include: (a) taking advantage of the spline interpolation package developed in [9] which can also find the tangential derivatives easily for a quantity defined on the interface. (b) better control of accuracy and area preservation since we have control of numbers of points on the interface. The main step to move the cell boundary from time level t^n to t^{n+1} are the following:

- Evaluate the interface information such as the tangential and normal directions, the jumps and their derivatives along the interface using the period spline interpolation package [9].

- Use the IIM method [7, 9, 10] to solve the Poisson equation for the pressure. With the IIM method, the discrete system of equations are standard Laplacian plus some correction terms at irregular grid points. The cost is just a little more than one call to the fast Poisson solver, which is the one from the Fish-pack in our method.

- Interpolate the pressure to get p_x and p_y including those grid points near or on the interface. The standard central finite difference schemes at a regular grid point (x_i, y_j) are

$$p_x = \frac{p_{i+1,j} - p_{i-1,j}}{2h}, \qquad p_y = \frac{p_{i,j+1} - p_{i,j-1}}{2h}.$$

  At an irregular grid point, we use the one-sided weighted least square interpolation [11] to get p_x and p_y. For example,

$$p_x(x_i, y_j) = \sum_{k,l} \beta_{kl}\, p_{kl}$$

  where the summation is taken for those points (x_k, y_l) that are in the same side of the interface as (x_i, y_j) and

$$(x_k - x_i)^2 + (y_l - y_j)^2 \le \delta^2$$

  for a given $\delta \sim Ch$, for some constant C. In our test, C is usually chosen as $3.6h$. Such interpolation gives smooth error distribution and better accuracy. Usually the system of equations for the interpolation coefficients are under-determined and is solved using the singular value decomposition process. Since the dimension of the system is small, such interpolation does not add much extra cost to the entire algorithm.

- Use the fast IIM method [11] to solve the elliptic equations with given jump conditions. Since there can be a big jump in the viscosity, such a solution process used to be the most expensive part. In the fast IIM method, we introduce an unknown jump $[u_n]$ which is only defined along those marked particle. A GMRES iteration is used to solve the unknown $[u_n]$. Each iteration of GMRES is one call to the fast Poisson solver. With the fast IIM method, the number of iterations is *independent* of both the jump in the coefficients and the mesh size. The fast IIM method takes advantage of the fast Poisson solver from the Fish-pack. It is almost impossible to simulate the problem discussed here with large jump in the viscosity without the fast IIM method. The fast IIM solver for elliptic interface problems with piecewise coefficients is available through the public ftp cite at North Carolina State University[1].

- Use the weighted least squares interpolation again to interpolate the velocity field at the marked points to get the velocity $\mathbf{U}_k^n$, $k = 1, 2, \cdots n_b$.

[1] ftp.ncsu.edu under the directory of */pub/math/zhilin/Package*.

- Update the cell boundary using the computed velocity

$$\mathbf{X}_k^{n+1} = \mathbf{X}_k^n + \Delta t\, \mathbf{U}_k^n, \quad k = 1, 2, \cdots n_b. \tag{3.27}$$

The time step for the explicit method is chosen as

$$\Delta t = \frac{h^2}{\max\limits_k |\mathbf{U}_k^n| \ \max\{\, \mu^+, \mu^- \,\}}. \tag{3.28}$$

While it is reasonable to use an explicit method for two dimensional simulation, an implicit method may be needed for three dimensional problems.

4 Numerical examples

All the calculations in this section were performed at North Carolina State University using Sun workstations. Most simulations are done within hours depending on the number of grid points. We use the spline interpolation package developed in [9] to express the interface.

4.1 Example 1.

We first test the classic case in which the surface tension γ is a constant. It is well known that the cell boundary will relax to a circle, its equilibrium state. The initial cell boundary is:

$$r(\theta) = 0.5 + 0.2\sin(5\theta), \quad 0 \le \theta \le 2\pi, \tag{4.29}$$

where $r = \sqrt{x^2 + y^2}$. The computational domain is $[-1,\ 1] \times [-1,\ 1]$.

We test our code for different viscosity and the surface tension. The numerical experiments reveal the following two important features. In Fig. 3, we plotted the evolution of the cell boundary with a 80 by 80 grid and $n_b = 80$ marked points on the cell boundary.

- We know that the larger the surface tension is, the faster the boundary restore to the equilibrium state, the circle with the same area as the original cell. In Fig. 3, we plotted the cell boundary at different time with different surface tension and the ratio μ^-/μ^+. In Fig. 3 (a) and (b), the surface tension is $\gamma = 0.01$, a small number, and it takes long time for the cell boundary to converge to or close to its equilibrium state. In Fig. 3 (c) and (d), the surface tension is $\gamma = 0.1$, we see the cell boundary moves much faster than the first case.

- Another factor that affects the motion of the cell boundary is the ratio μ^-/μ^+, where μ^+ and μ^- are the viscosity of the fluids outside and inside of the cell boundary, respectively. The larger this ratio is, the faster of the motion. In Fig. 3 (a) and (c), the ratio is one and we see slower motion compared with Fig. 3 (b) and (d) even if the surface tension is the same.

The algorithm is quite accurate in the sense that the symmetry and the area are both preserved very well. In all cases, the relative area change is less than 4%. The largest area changes are from first a few steps since the initial cell boundary has pretty large curvature. In the figure, E_{area} is the relative error in the area at that particular time.

4.2 Example 2

In this test, we try to use a non-linear surface tension to simulate the cell cleavage similar to those described in [1, 2, 3]. However, we are dealing with two phases instead of one. First we test the case that is similar to the numerical test in [3] and analyzed in [1, 2]. The initial cell boundary is a circle

$$x^2 + y^2 = 0.45^2.$$

The surface tension is chosen as

$$\tau = 0.01 + \epsilon\, \delta_w(x(s)), \tag{4.30}$$

where $x(s)$ is the x-coordinates of the cell boundary, and $\delta_w(x)$ is defined as

$$\delta_w(x) = \begin{cases} \dfrac{1}{4w}\left(1 + \cos\left(\pi x/2w\right)\right), & \text{if } |x| < 2w, \\ 0, & \text{if } |x| \geq 2w, \end{cases} \tag{4.31}$$

the discrete delta function for the immersed boundary method [14]. According to the theory in Greenspan [1, 2] and verified by He and Dembo in [3], the cell will bend in the middle which is again confirmed by our numerical example. In Fig. 4, we plotted the cell boundary at $t = 0$ and $t = 68.125$ for the case of equal viscosity, and $t = 18.2807$ for the case of different viscosity $\mu^+ = 0.01$ and $\mu^- = 1$. While the choice of the non-linear surface tension will affect the deformation of the cell, our numerical experiments agree with the conclusion in [3] that the cell can not have large deformation if (4.30) is used. In fact, for two dimensional problem, the boundary will stop move further if the curvature is zero, and the boundary reaches its equilibrium state.

In order to have a cell deform further, some different surface tension should be used in the model (1.1)-(1.3). We use the following surface tension

$$\tau = 0.01 - \epsilon\, \delta_w(x(s)). \tag{4.32}$$

Note that this is similar to the generalized Gibbs-Thomson condition, see [6] and the references therein. The initial cell boundary is the circle $r = 0.45$ with a perturbation:

$$r(\theta) = 0.45 + 0.15\cos 2\theta, \quad 0 \leq \theta \leq 2\pi. \tag{4.33}$$

This can be interpreted as the follows: In some small part of the cell boundary, there is sudden change in the concentration of the material due to, for example, chemical reaction.

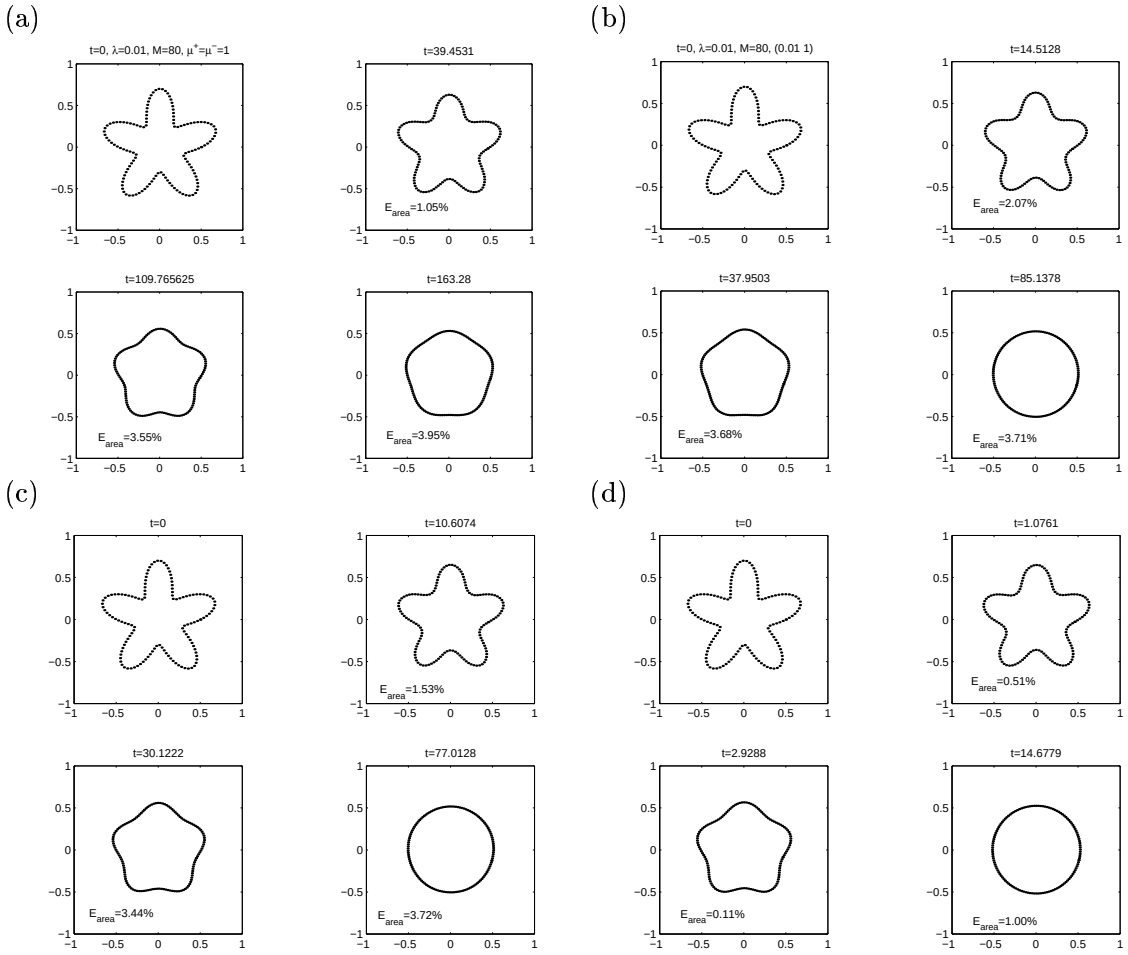

Figure 3: The cell boundary at different time computed using a 80 by 80 grid and a constant surface tension $\gamma = 0.01$ in (a) and (b), and $\gamma = 0.1$ in (c) and (d). While the boundary in all cases approaches to the equilibrium state, a circle, the time scale is very different. The boundary moves faster as γ or the ration μ^-/μ^+ gets larger. (a) The result with equal viscosity $\mu^- = \mu^+ = 1$, and $\gamma = 0.01$ at time $t = 0$, $t = 39.4531$, $t = 109.7656$, and $t = 163.28$. The shape is far away from the equilibrium state even with $t = 163$. (b) The result with different viscosity $\mu^- = 1$, $\mu^+ = 0.01$, and $\gamma = 0.01$ at time $t = 0$, $t = 14.5128$, $t = 37.9503$, and $t = 85.1378$. The shape is very close to the equilibrium state at $t = 85$. So the motion is much faster than the case with equal viscosity. (c) The result with equal viscosity $\mu^- = \mu^+ = 1$, and $\gamma = 0.1$ at time $t = 0$, $t = 10.6074$, $t = 30.1222$, and $t = 77.0128$. The motion is faster than the case with small surface tension but slower than the case with larger ratio of μ^-/μ^+. (d) The result with different viscosity $\mu^- = 1$, $\mu^+ = 0.01$, and $\gamma = 0.1$ at $t = 0$, $t = 1.0761$, $t = 2.9288$, and $t = 14.6779$. The motion is faster than any other three cases in this figure.

(a) (b)

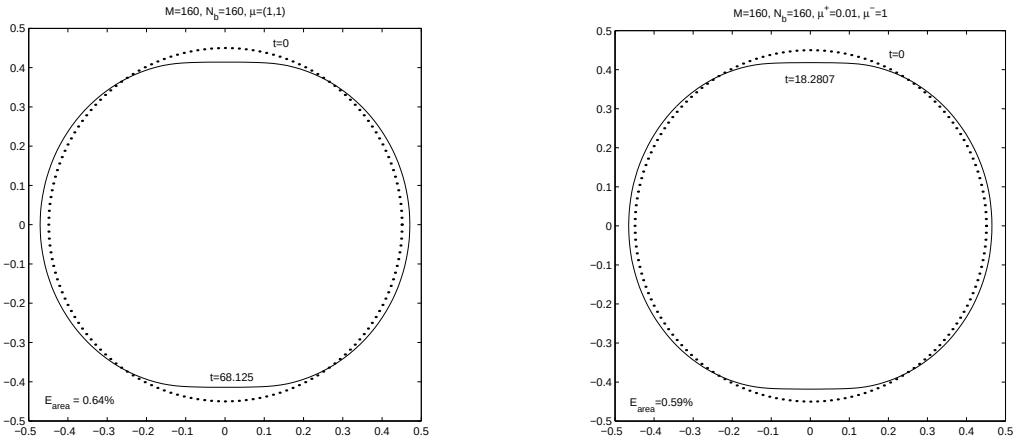

Figure 4: The cell boundary at different time. The dotted plot is the initial cell boundary which is the circle $r = 0.45$. The surface tension is given in (4.30). (a) The solid line is the cell boundary at $t = 68.125$ in the case of equal viscosity $\mu^+ = \mu^- = 1$. The relative area change at $t = 68.125$ is 0.64%. (b) The solid line is the cell boundary at $t = 18.2807$ is the case of different viscosity $\mu^+ = 0.01$ and $\mu^- = 1$. The relative area change at $t = 18.2807$ is 0.59%. Again the motion is faster when the ratio μ^-/μ^+ is larger.

(a) (b)

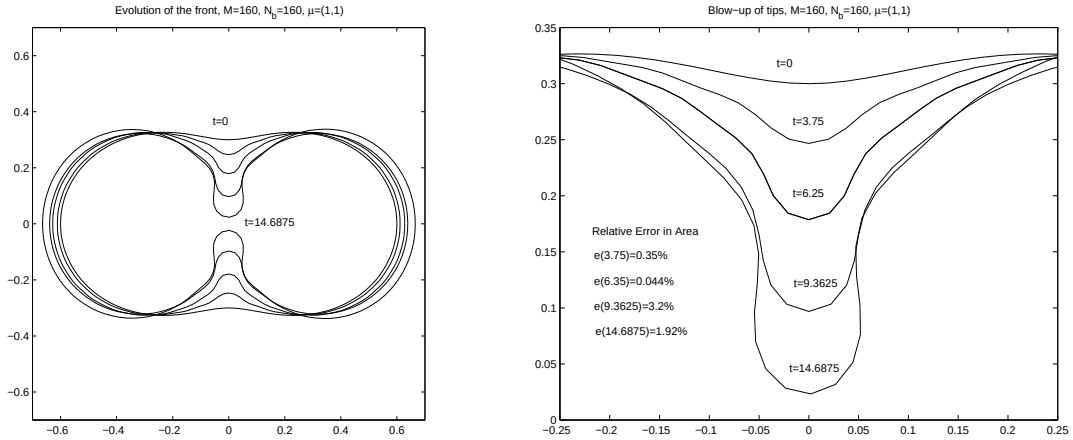

Figure 5: The evolution of the cell boundary for for Example 3 with equal viscosity $\mu^+ = \mu^- = 1$ at different time. (b) Blow-up of the upper tip. The relative area changes at different time are also listed in the figure.

As the result, the cell will gradually deform as observed in the experiments. In Fig. 5, we plotted the evolution process of the cell boundary with equal viscosity $\mu^+ = \mu^- = 1$, $w = 5h$, and $\epsilon = h$, where $h = (b-a)/M = (d-c)/N$, is the spatial step size. We see that cell is dividing and eventually will break up. The simulation is done with a 160 by 160 grid and 160 marked points on the cell boundary. Fig. 5 (b) is the blow-up plot of the upper tip. The area changes which is also marked on the figure, are relatively small, less than 3.2%, for such a problem with the tips deepening so much in both directions. In Fig. 6, we plotted the simulation with different viscosity $\mu^+ = 0.01$ and $\mu^- = 1$, we see similar behavior as the case of the equal viscosity but faster motion as we discussed for Example 1.

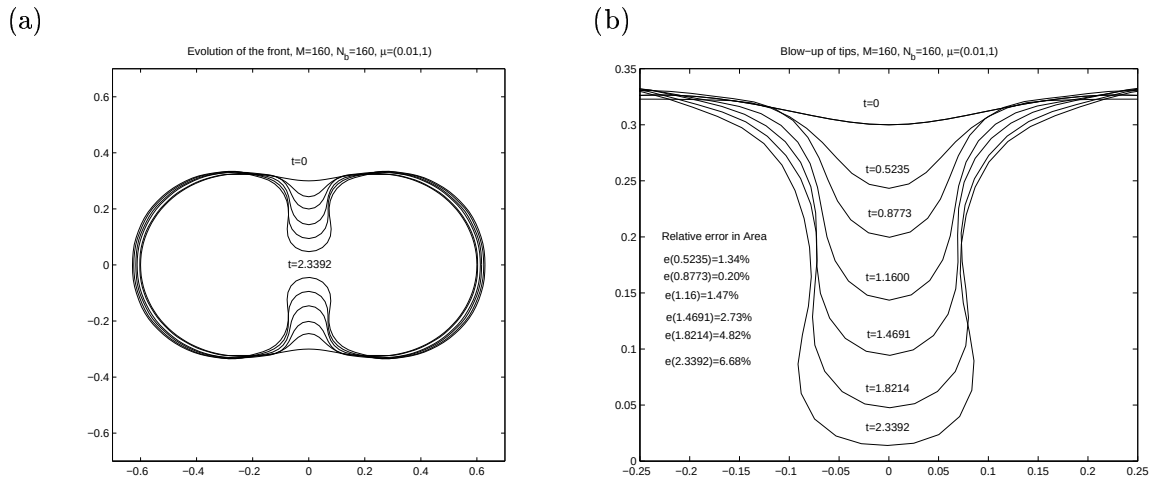

Figure 6: The evolution of the cell boundary for for Example 2 with different viscosity $\mu^+ = 0.01$ and $\mu^- = 1$ at different time. (b) Blow-up of the upper tip. The relative area changes at different time are also listed in the figure. The motion is faster than the case of the equal viscosity.

5 Conclusion.

We have developed a finite difference method for Stokes equations for incompressible two-phase flow that models cell deformation with discontinuous viscosity and non-linear surface tension. The decoupled jump conditions for the pressure and the velocity across the cell boundary are crucial for the success of the new-developed algorithm. With similar choice of the surface tension, our numerical results agree with the results and analysis in the literature. Our numerical results also showed that with suitable choice of surface tension, a cell can deform and break-up. While it is known that motion of a cell boundary depends on the surface tension, our numerical experiments also showed that the motion depends on the difference of the viscosity as well.

Future work we intend to study including: (a) design implicit scheme so that we can use larger time steps. (b) Three dimensional and axisymmetric simulations. (c) Optimal choice of the surface tension to match certain patterns of cell deformations.

Acknowledgments

The first author was partially supported by an NSF grant DMS0073403; and an ARO under grant number 39676-MA. We would like to thank Dr. Xiaobiao Lin for useful discussions.

References

[1] H. P. Greenspan. On the deformation of a viscous droplet caused by variable surface tension. *Studies in Applied Mathematics*, 57:45–58, 1977.

[2] H. P. Greenspan. On the dynamics of cell cleavage. *J. Theor. Biol.*, 65:79–99, 1977.

[3] X. He and M. Dembo. Numerical simulation of oil-droplet cleavage by surfactant. *J. Biomechanical Engineering*, 118:201–209, 1996.

[4] D. D. Joseph and Y. Y. Renardy. *Fundamentals of two-fluid dynamics.* Springer-Verlag, 1993.

[5] M-C. Lai and Z. Li. A remark on jump conditions for the three-dimensional navier-stokes equations involving an immersed moving membrane. *Applied Math. Letters*, in press, 2000.

[6] P. H. Leo, J. S. Lowengrub, and Q. Nie. Miscrostructural evolution in orthotropic elastic media. *J. Comput. Phys.*, 157:44–88, 2000.

[7] R. J. LeVeque and Z. Li. The immersed interface method for elliptic equations with discontinuous coefficients and singular sources. *SIAM J. Numer. Anal.*, 31:1019–1044, 1994.

[8] R.J. LeVeque and Z. Li. Immersed interface method for Stokes flow with elastic boundaries or surface tension. *SIAM J. Sci. Comput.*, 18:709–735, 1997.

[9] Z. Li. *The Immersed Interface Method — A Numerical Approach for Partial Differential Equations with Interfaces.* PhD thesis, University of Washington, 1994.

[10] Z. Li. A note on immersed interface methods for three dimensional elliptic equations. *Computers Math. Appl.*, 31:9–17, 1996.

[11] Z. Li. A fast iterative algorithm for elliptic interface problems. *SIAM J. Numer. Anal.*, 35:230–254, 1998.

[12] Z. Li and K. Ito. Maximum principle preserving schemes for interface problems with discontinuous coefficients. *NCSU CRSC-TR00-04*, 2000.

[13] J. R. Lister. Capillary breakup of a viscous thread surrounded by another viscous fluid. *Physics of fluids*, 10:2758–2764, 1998.

[14] C. S. Peskin. Numerical analysis of blood flow in the heart. *J. Comput. Phys.*, 25:220–252, 1977.

[15] C. S. Peskin and D. M. McQueen. A general method for the computer simulation of biological systems interacting with fluids. *Symposia of the Society for Experimental Biology*, 49:265, 1995.

[16] J. M. Rallison and A. Acrivos. A numerical study of the deformation and burst of a viscous drop in an extensional flow. *J. Fluid Mech.*, 89:191–200, 1978.

[17] H. A. Stone and L. G. Leal. The effect of surfactants on drop deformation and breakup. *J. Fluid Mech.*, 220:161–186, 1990.

[18] C. Tu and C. S. Peskin. Stability and instability in the computation of flows with moving immersed boundaries: a comparison of three methods. *SIAM J. Sci. Stat. Comput.*, 13:1361–1376, 1992.